České vysoké učení technické v Praze, Fakulta strojní

Czech Technical University in Prague, Faculty of Mechanical Engineering

Ing. Jan Halama, Ph.D.

Numerické řešení transsonického proudění kondenzující páry v dýze a v turbínách

Numerical Solution of Transonic Flow of Condensing Steam in Nozzle and Turbines

Summary

This lecture is aimed at numerical modeling of transonic flow of condensing steam, which occurs in steam turbines. Presented flow model is based on the model published in [17]. Several extensions of the model including surface tension correction, alternative equation of state and droplet size spectra reconstruction are discussed. Problem formulation and boundary condition description are presented. Results have been obtained by author's own numerical code based on the fractional step method, which links a finite volume method for the convection terms with the Runge-Kutta method for the production terms. Numerical results of several flow problems including the steady flow in a convergent-divergent nozzle, the steady flow in a turbine cascade and the unsteady stator-rotor interaction in a turbine stage are presented. Comparison of numerical results with experimental data for the flow in a nozzle is included.

Souhrn

Tato přednáška je zaměřena na numerické modelování transsonického proudění páry v turbínách. Uvedený model proudění vychází z modelu publikovaného v [17]. Jsou diskutována rozšíření původního modelu, která se týkají korekce povrchového napětí vody, alternativní stavové rovnice pro páru a rekonstrukce spektra velikostí kapek. Je uvedena formulace úlohy a jsou popsány okrajové podmínky. Numerické výsledky byly získány metodou, která je založena na metodě rozkladu operátoru a která využívá metodu konečných objemů pro diskretizaci konvekčních členů a Rungovu-Kuttovu metodu pro integraci produkčních členů. Ukázky numerických výsledků zahrnují případy stacionárního proudění v Lavalově dýze, stacionárního proudění v turbínové mříži a nestacionární interakce statoru a rotoru v turbínovém stupni. Numerické výsledky proudění v dýze jsou porovnány s experimentálními daty.

Klíčová slova: transsonické proudění, mokrá pára, metoda konečných objemů, homogenní nukleace, kondenzační ráz, parní turbína.

Keywords: transonic flow, wet steam, finite volume method, homogeneous nucleation, condensation shock, steam turbine.

Contents

1 Introduction

The first attempt to use steam as a working fluid is probably dated to the 1st century. Heron from Alexandria invented a well recognized steam-powered device called an Aeolipile working on the reaction principle of steam flow. Thomas Newcomen used the pressure drop of condensed saturated steam to drive a water pump in the 18th century. This pump was improved by James Watt, who later designed well known steam engine, which started the boom of industry and transportation. Nowadays, one of the most important application for steam flow is a steam turbine used mainly for the production of electric power. A thermodynamics of such process corresponds to the Rankin cycle. To have highly efficient large power turbine, one wants to design a turbine with big pressure and temperature gradient. The pressures and the temperatures of steam coming from boiler to the inlet of turbine can be as high as 20 MPa and 1000 K respectively and the pressure at the exit from turbine is below the atmospheric pressure. During such expansion an initially dry steam condensates. The condensation is a non-equilibrium process, which starts when the vapor temperature decreases sufficiently below the saturation temperature. The vapor with the temperature below the saturation temperature and before condensation start is in the so called metastable state. The condensation in a turbine has different mechanisms. The liquid phase can appear suddenly in a form of very small droplets dispersed in vapor, this phenomena is called nucleation. There is the homogeneous nucleation, where droplets start to grow from clusters of water molecules and the heterogenous nucleation where vapor starts to condensate on some particles present in vapor. Another mechanism of condensation is a film condensation on surfaces of inner structures of turbine. Droplets of liquid already present in the steam can grow or evaporate according to the state of surrounding steam. The presence of liquid phase leads to a very complex two-phase flow of mixture of vapor and liquid droplets. The mixture contains droplets with a very big range of sizes. The droplets appearing due to homogenous nucleation have sub-micron size and are convected by the vapor. Droplets appearing due to liquid film separation are much bigger and they have different velocity then the vapor. On top of this, condensation usually starts in a low pressure part of turbine with blades usually longer than one meter and due to the rotational speed of turbine (given by the AC voltage frequency 50Hz) the tip circumferential speed of last rotors is supersonic. It is well known that supersonic flow is very sensitive on the latent heat release due to condensation. This released heat changes significantly shock wave structure and may also induce pressure oscillations. Moreover the combination of high velocities and the presence of droplets of different sizes in the flow field leads to blade erosion phenomena. The condensation also decreases the thermal efficiency of turbine. There are technical solutions like local re-heating and condensed water separation, which try to minimize the undesired effects of condensation. All of these phenomena makes the design of steam turbine challenging. Research of non-equilibrium condensation is difficult. Experimental as well as numerical studies are based on certain level of assumptions and approximations. Experiments rely often on indirect methods, e.g. light scattering methods. Numerical simulations, on the other hand, are often based on simplified thermodynamic models of steam and approximations of droplet size spectra. Despite all of these issues numerical simulations together with experimental tests help to get better insight in condensation phenomena and contribute to design of steam turbines.

Numerical simulations of two-phase flow of steam have evolved over three decades. The first simulations of two-dimensional two-phase flow in turbine cascade e.g. [2], [1], [11] or [19] were based on the solution of flow field in the Eulerian framework and wetness

(homogeneous nucleation and droplet growth) was calculated along streamlines in the Lagrangian framework. The advantage of this algorithm is that condensation is solved as the one-dimensional problem along streamline with known expansion and allows to track the complete history of droplets. The main disadvantage is the need to recompute streamlines every n-th iteration of time-marching algorithm. Later works are based mainly on fully Eulerian approach, where transport equations for mass, momentum and energy of the mixture are supplemented by transport equations for additional parameters of liquid phase. Models based on the assumption of monodispersity of mixture contain transport equations for the total mass and the total number of droplets e.g. [8], [5], [6], [7] or [16]. Models based on the method of moments [9] are able to recognize the polydispersity of mixture. There are works, where moments are used to compute the average droplet size only, e.g. [14] and works, where moments are used to reconstruct the droplet size distribution, e.g. [12] or [10]. Most of simulations consider that droplets are convected by the vapor. Recent paper [18] present the use of two-fluid single-pressure flow model for the simulation of transonic flow of condensing steam in a nozzle. The observation is, that small droplets coming from nucleation have velocity very similar to the velocity of vapor. Such model could be possibly used for modeling of flow of mixture with bigger droplets coming e.g. from liquid film separation. The research of film condensation modeling is open and can be one of the future directions towards more complex simulations.

2 Model of wet steam flow

Presented model of wet steam flow originates from the model [17]. The vapor specific heat ratio, considered as a constant in [17], is taken as a function of vapor temperature. The homogenous nucleation model is supplemented by the correction term published in [13]. The model is closed by the polynomial functions for the material properties of water taken from [8]. The velocity, pressure and temperature of steam is considered within the range typical for the flow in a steam turbine. Condensed water, if it is present, is dispersed in vapor in the form of high amount of small spherical droplets, therefore the velocity of droplets is considered to be the same as the velocity of vapor. The flow model is based on the conservation laws for mass, momentum and energy of the mixture and for the mass fraction of liquid phase. Mass exchange between vapor and droplets is given by the models of homogeneous nucleation and droplet growth. The whole spectra of droplet sizes in the elemental volume of mixture is described by the three moments according to [9]. Such model is able to describe polydispersity of mixture and can be complemented by some model of distribution of droplet size. The moments are

$$Q_0 = N, \qquad Q_1 = \sum_{i=1}^{N} r_i, \qquad Q_2 = \sum_{i=1}^{N} r_i,^2 \tag{1}$$

where N denotes the total number of droplets per unit mass and r_i is the radius of $i-th$ droplet. The average droplet radius is approximated by $\overline{r} = \sqrt{Q_2/Q_0}$ if the wetness χ is above a chosen minimum χ_{min} otherwise it is set $\overline{r} = 0$ to avoid numerical errors. The full system of transport equations for three-dimensional flow in integral form for arbitrary control volume V_k reads

$$\frac{\partial}{\partial t} \iiint\limits_{V_k} \mathbf{W} \, dV + \oint\limits_{\partial V_k} \left(\mathbf{F}(\mathbf{W}), \mathbf{G}(\mathbf{W})\right) \vec{n}_{\partial V_k} dS = \iiint\limits_{V_k} \mathbf{Q}(\mathbf{W}) dV \tag{2}$$

$$\mathbf{W} = \begin{bmatrix} \rho \\ \rho u \\ \rho v \\ e \\ \rho\chi \\ \rho Q_2 \\ \rho Q_1 \\ \rho Q_0 \end{bmatrix}, \quad \mathbf{F}^c = \begin{bmatrix} \rho u \\ \rho u^2 + p \\ \rho uv \\ (e+p)u \\ \rho\chi u \\ \rho Q_2 u \\ \rho Q_1 u \\ \rho Q_0 u \end{bmatrix}, \quad \mathbf{F}^v = \begin{bmatrix} 0 \\ \tau_{xx} \\ \tau_{xy} \\ u\tau_{xx} + v\tau_{xy} - q_x \\ 0 \\ 0 \\ 0 \\ 0 \end{bmatrix},$$

$$\mathbf{G}^c = \begin{bmatrix} \rho v \\ \rho vu \\ \rho v^2 + p \\ (e+p)v \\ \rho\chi v \\ \rho Q_2 v \\ \rho Q_1 v \\ \rho Q_0 v \end{bmatrix}, \quad \mathbf{G}^v = \begin{bmatrix} 0 \\ \tau_{xy} \\ \tau_{yy} \\ u\tau_{xy} + v\tau_{yy} - q_y \\ 0 \\ 0 \\ 0 \\ 0 \end{bmatrix}, \quad \mathbf{Q} = \begin{bmatrix} 0 \\ 0 \\ 0 \\ 0 \\ \frac{4}{3}\pi r_c^3 J\rho_l + 4\pi\rho\mathcal{M}_2\rho_l \\ r_c^2 J + 2\rho\mathcal{M}_1 \\ r_c J + \rho\mathcal{M}_0 \\ J \end{bmatrix},$$

$$\mathbf{F} = \mathbf{F}^c - \mathbf{F}^v, \quad \mathbf{G} = \mathbf{G}^c - \mathbf{G}^v, \quad \mathcal{M}_n = \int_0^\infty r^n N(r)\dot{r}(r)dr,$$

where $\vec{n}_{\partial V_k}$ is the outer unit normal vector of ∂V_k, ρ is the mixture density, u and v the mixture velocity components, e the total energy of mixture in unit volume, p is the pressure of the mixture, χ denotes the mass fraction of liquid phase, known also as wetness, J is the number of new droplets due to homogenous nucleation per unit volume per second, which have the size of critical radius r_c. The variable ρ_l denotes the density of liquid phase, $N(r)$ denotes the droplet size distribution function. The integral of $N(r)$ along the interval $< r_1, r_2 >$ gives the total number of droplets with the radius between r_1 and r_2 per unit mass of mixture. The function $\dot{r}(r)$ gives the droplet growth velocity of droplet with radius r. Provided the solution of (2) is sufficiently smooth one can derive the differential form

$$\frac{\partial \mathbf{W}}{\partial t} + \frac{\partial \mathbf{F}(\mathbf{W})}{\partial x} + \frac{\partial \mathbf{G}(\mathbf{W})}{\partial y} = \mathbf{Q}(\mathbf{W}). \tag{3}$$

However it is known, that discontinuous solutions are of practical importance (shock waves, contact discontinuities, etc.), therefore the integral form (2), which allows discontinuous solutions, is preferred. Moreover the balance of mass, momentum, energy and parameters of liquid phase from the point of view of arbitrary volume V_k is more natural for the development of a finite volume method. The system (2) has more unknowns than the number of equations, it has to be closed by additional equations related to properties of considered fluid. Under perfect gas assumption the equation for pressure reads

$$p = \frac{(\gamma - 1)(1 - \chi)}{1 + \chi(\gamma - 1)} \left[e - \frac{1}{2}\rho(u^2 + v^2 + w^2) + \rho\chi L \right], \tag{4}$$

where common pressure for both phases is considered and L denotes the latent heat of condensation/evaporation Further details are provided in [14] or [24]. The specific heat ratio is taken as a function of temperature

$$\gamma = \frac{c_p(T)}{c_p(T) - R_v}, \tag{5}$$

where R_v is the gas constant for vapor, c_p the specific heat at constant pressure c_p and T the vapor temperature. The system (2) models also the single-phase flow of vapor if $\chi = Q_0 = Q_1 = Q_2 = 0$. We assume two approximations of droplet growth speed $\dot{r}(r)$. The first one considers that the droplet growth speed depends only on average radius $\overline{r}$. The integrals in the source term $\mathbf{Q}$ are then replaced by a simple product

$$\mathcal{M}_n = \int_0^\infty r^n N(r)\dot{r}(\overline{r})dr = \dot{r}(\overline{r}) \int_0^\infty r^n N(r)dr = \dot{r}(\overline{r})Q_i. \tag{6}$$

Such model is denoted as AVG-P model. The second approximation considers certain reconstruction of the droplet size distribution function $N(r)$ from the values of moments Q_i. The model further denoted as DSDF-P is based on the log-normal distribution for $N(r)$, which can be obtained from three moments Q_0, Q_1 and Q_2, for details see [10] and [25].

$$N(r) = Q_0 \frac{1}{r \ln(\sigma_g)\sqrt{2\pi}} \exp\left(-\frac{\ln^2(r/\overline{r_g})}{2\ln^2(\sigma_g)}\right), \tag{7}$$

where

$$\overline{r_g} = \frac{\overline{r}}{\exp(0.5\ln^2(\sigma_g))}, \qquad \sigma_g = \exp\sqrt{\ln(c_v^2+1)},$$
$$\overline{r} = \sqrt{\frac{Q_2}{Q_0}}, \qquad c_v = \sqrt{\frac{Q_0 Q_2}{Q_1^2} - 1}. \tag{8}$$

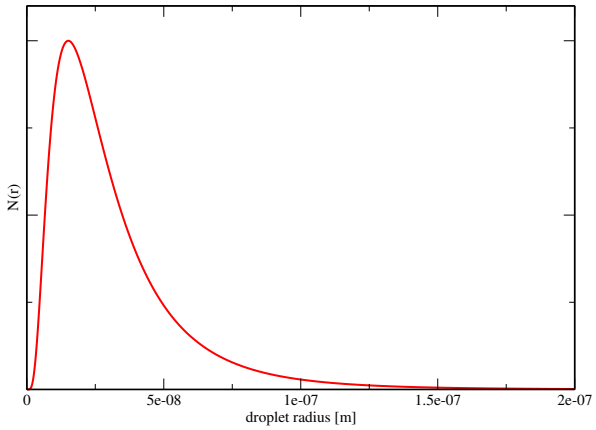

Figure 1: Example of log-normal droplet size distribution used in [25].

The model has been also successfully tested with alternative equation of state for steam from [16]

$$\frac{p}{\rho_v T} = R_v\left(1 + B\rho_v + C\rho_v^2\right). \tag{9}$$

The variables T and ρ_v denote the temperature and the density of vapor respectively, the pressure p is considered the same for both phases. Models with this equation of state are denoted as the AVG-V and the DSDF-V models.

The number of new droplets due to homogenous nucleation per second and per unit volume is computed using a classical formula [4]

$$J = \sqrt{\frac{2\sigma}{\pi m_v^3}} \cdot \frac{\rho_v^2}{\rho_l} \cdot \exp\left(-\beta \cdot \frac{4\pi r_c^2 \sigma}{3 k_B T}\right), \tag{10}$$

where the surface tension σ of water is a function of temperature and β is the correction coefficient proposed in [13]

$$\beta = 1.328 p_{cor}^{0.3}, \quad p_{cor} = p_{saturated}(s_{01}) 10^{-5}, \tag{11}$$

where s_{01} is the entropy corresponding to the inlet total conditions and p_{cor} is considered in $[bar]$ unit. This correction is applied for the AVG-P and DSDF-P models based on the perfect gas assumption in order to match the onset of nucleation. This correction is not needed for models AVG-V and DSDF-V. The new droplet appearing due to homogenous nucleation has the initial radius equal to the critical radius

$$r_c = \frac{2\sigma}{L\rho_l \ln(T_s/T)}, \tag{12}$$

where $L(T)$ is the latent heat of condensation/evaporation and $\rho_l(T)$ denotes the density of water. The saturation temperature T_s is evaluated according to IAPWS-IF97 formulation. An existing droplet is growing or it can also evaporate depending on the vapor temperature. We consider the Gyarmathy's droplet growth model

$$\dot{r}(r) = \frac{\lambda_v (T_s - T)}{L\rho_l (1 + 3.18 \cdot Kn)} \cdot \frac{r - r_c}{r^2}, \qquad Kn = \frac{\eta_v \cdot \sqrt{2\pi R_v T}}{4rp}, \tag{13}$$

where vapor thermal conductivity λ_v and vapor viscosity η_v are functions of temperature and r is the droplet radius. Critical radius r_c goes to infinity for vapor temperature approaching the saturation temperature. This growth is compensated by the term $(T_s - T)$, which is going to zero at the same time, so $\dot{r}(r)$ remains finite, however direct implementation of the Eq. (13) is dangerous, since the product of 'almost infinity' with 'almost zero' has unpredictable behavior. Therefore we implement the formula (14)

$$\dot{r}(r) = \frac{\lambda_v}{L\rho_l (1 + 3.18 \cdot Kn)} \left(\frac{T_s - T}{r} - \frac{2\sigma}{L\rho_l r^2} \cdot \frac{T_s - T}{\ln \frac{T_s}{T}}\right), \tag{14}$$

where the term $\dfrac{T_s - T}{\ln \frac{T_s}{T}}$ ('zero' divided by 'zero' for T going to T_s) is approximated using Taylor expansion

$$\frac{T_s - T}{\ln \frac{T_s}{T}} = T \frac{\frac{T_s}{T} - 1}{\ln \frac{T_s}{T}} = 1 + \frac{1}{2}\vartheta - \frac{1}{12}\vartheta^2 + \frac{1}{24}\vartheta^3 - \frac{19}{720}\vartheta^4 + \frac{3}{160}\vartheta^5, \quad \vartheta = \frac{T_s}{T} - 1. \tag{15}$$

The later implementation of droplet growth formula yields a stable numerical algorithm also for cases with steam parameters close to saturation line.

3 Problem formulation

Designers of turbines use several types of flow simulations ranging from one- to three-dimensional cases. An important role has a through-flow simulation of two-dimensional circumferentially averaged flow, which is used to compute span-wise distributions of flow-field parameters upstream and downstream each considered blade row. Another frequent simulation is the simulation of two-dimensional flow in a blade to blade plane 'parallel' to hub or shroud, which is used to predict a performance of blade profile and which corresponds to experimental setup for plane cascade. One of the most complex are simulations of three-dimensional steady flow in a cascade or even unsteady flow in single/multiple stage setup.

The problem formulated for the system (2) or (3) is a non-linear problem, which is still not fully covered by mathematical theory of existence and uniqueness of solution. The choice of boundary and initial conditions is based on the properties of linearized model and also on the best practice knowledge. Let explain a typical problem formulation for two cases of two-dimensional flow in a nozzle or single blade channel of plane cascade, see the Fig. 2.

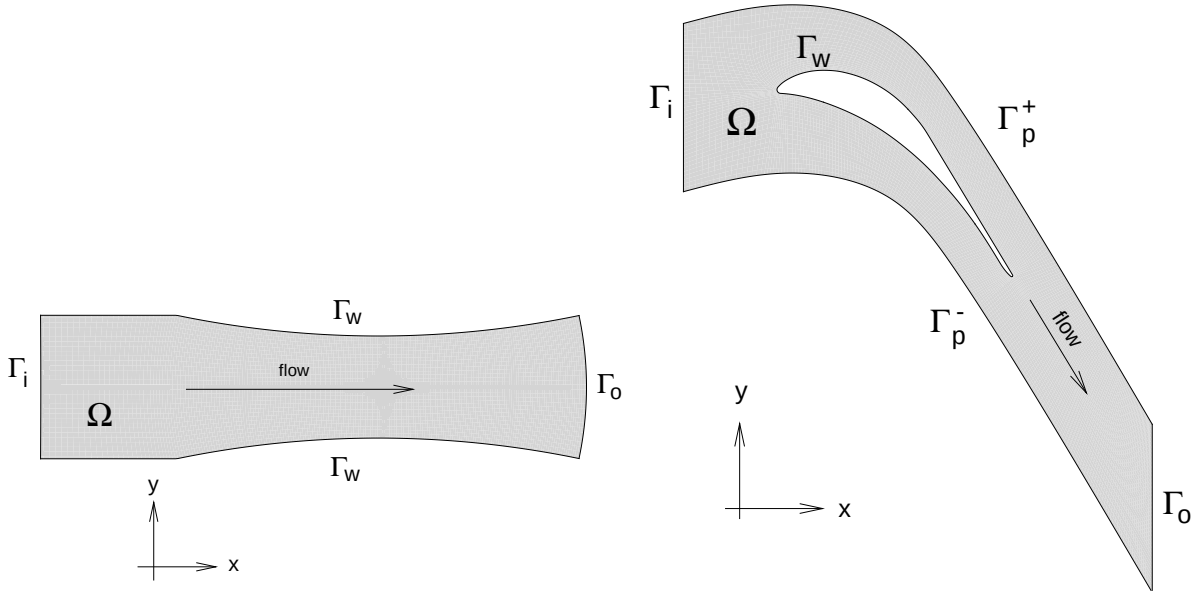

(a) nozzle (b) turbine cascade

Figure 2: Examples of solution domains.

The following boundary conditions are used for the inviscid flow model. Consider flow, which is subsonic in the perpendicular direction to the inlet boundary Γ_i and which enters the solution domain Ω in each point of the inlet boundary Γ_i (one has to avoid recirculating flow). Then 'the number of unknowns minus one' parameters have to be set according to the 1D theory of characteristics of linearized problem. We prescribe a constant values of reservoir conditions T_0 and p_0, the flow direction, χ, Q_0, Q_1 and Q_2. The non-permeability condition $(u, v)\vec{n} = 0$, where $\vec{n}$ denotes the normal vector to boundary, is considered along walls Γ_w. The flow in the perpendicular direction to the outlet boundary Γ_o is typically subsonic for turbine cascade, therefore according to the 1D theory of characteristics for linearized problem one parameter has to be specified. It is natural to prescribe a value of outlet pressure. Because of possible presence of pressure gradient along the outlet boundary Γ_o it is better to fix only the mean value of pressure

and to let the pressure profile compute as a results of simulation. This condition allows shock wave passing through outlet boundary. However the fixed mean value of pressure works well only for steady flow, the constant distribution of pressure has to be used for unsteady flow. The homogeneous Neumann's condition for the temperature has to be added in the case of unsteady two-phase flow to avoid temperature oscillations. The flow in the perpendicular direction to the outlet boundary Γ_o of nozzle can be supersonic, in such case there is no boundary condition along Γ_o. The computational domain for turbine flow calculations consists usually of one blade passage, i.e. a spatial periodicity of solution is considered, i.e. $\mathbf{W}_{\Gamma_p^-}(x) = \mathbf{W}_{\Gamma_p^+}(x)$. The boundary conditions for viscous flow are similar, the system of the above mentioned conditions is completed by proper Neumann's conditions. The non-permeability condition along walls is of course replaced by the no-slip condition $u = 0,\ v = 0$ and the adiabatic wall condition $\partial T/\partial \vec{n} = 0$. The equation (2) describes the time evolution of $\mathbf{W}$ from given initial condition. We are interested in two types of solution. The first one is the steady solution, which is obtained as a limit of $\mathbf{W}$ for $t \to \infty$ provided all boundary conditions are time independent (time marching method). The second type is time dependent periodic solution, which is obtained also as a certain limit of $\mathbf{W} = \mathbf{W}_{transient} + \mathbf{W}_{periodic}$ for sufficiently large t to satisfy $\|\mathbf{W}_{transient}\| \to 0$ provided all boundary conditions are periodic in time.

4 Numerical method

The numerical method has to cover very different time scales of convection, nucleation and droplet growth. Numerical method is therefore based on the symmetrical splitting method [15], which allows separate solution of each phenomena by individual numerical method. The original problem for the system (2) is approximated by the solution of three successive sub-problems

$$\frac{\partial}{\partial t} \iint\limits_{V_k} \mathbf{W}^* \, dV = \iint\limits_{V_k} \mathbf{Q}(\mathbf{W}^*) dV \tag{16}$$

$$\frac{\partial}{\partial t} \iint\limits_{V_k} \mathbf{W}^{**} \, dV = - \oint\limits_{\partial V_k} \left(\mathbf{F}(\mathbf{W}^{**}), \mathbf{G}(\mathbf{W}^{**})\right) \vec{n}_{\partial V_k} dS \tag{17}$$

$$\frac{\partial}{\partial t} \iint\limits_{V_k} \mathbf{W}^{***} \, dV = \iint\limits_{V_k} \mathbf{Q}(\mathbf{W}^{***}) dV \tag{18}$$

where the equation (16) is solved with initial data $\mathbf{W}^*(t) = \mathbf{W}(t)$. The advance $\Delta t/2$ in time for the solution of (16) yields the initial data for the equation (17), i.e. $\mathbf{W}^{**}(t) = \mathbf{W}^*(t + \Delta t/2)$. Then the shift Δt in time for the solution of (17) yields the initial data for the equation (18), i.e. $\mathbf{W}^{***}(t) = \mathbf{W}^{**}(t + \Delta t)$. The time shift $\Delta t/2$ for the solution of (18), i.e. $\mathbf{W}^{***}(t + \Delta t/2)$, corresponds to the time shift Δt for the solution $\mathbf{W}(t + \Delta t)$ of the original un-split system (2). The single step of Lax-Wendroff finite volume method is applied for (17) and several steps of Runge-Kutta method evaluate the source term contribution in (16) and (18). The algorithm of the splitting method reads

$$\begin{aligned} \mathbf{W}_K^{(j+1)} &= \mathcal{RK}(\mathbf{W}_K^{(j)}, \frac{\Delta t}{2m}),\ j = 0, \ldots, m-1 \\ \mathbf{W}_K^{(m+1)} &= \mathcal{FV}(\mathbf{W}_K^{(m)}, \Delta t) \\ \mathbf{W}_K^{(j+1)} &= \mathcal{RK}(\mathbf{W}_K^{(j)}, \frac{\Delta t}{2m}),\ j = m+1, \ldots, 2m \end{aligned} \tag{19}$$

where $\mathbf{W}_K^{(0)} = \mathbf{W}_K^n$, $\mathbf{W}_K^{n+1} = \mathbf{W}_K^{(2m+1)}$, $\mathcal{FV}(\mathbf{W}_K^n, \Delta t)$ denotes one step of finite volume method (Lax-Wendroff, CFFV, SRNH method) with initial data $\mathbf{W}_K^n$ and time step Δt (subscript $\cdot_K$ denotes the K-th cell and superscript $\cdot^n$ the n-th time level). Similarly $\mathcal{RK}(\mathbf{W}_K^n, \Delta t)$ denotes one step of the Runge-Kutta method. The local number of substeps is $m = \Delta t/\tau$, where τ is the time scale of condensation and Δt is the time step of the finite volume method for the equation (17).

Due to the stability problems of the fully explicit method in three-dimensional case, the explicit method for the parts (16) and (18) has been replaced by the implicit Euler method. The nonlinear equation is solved by iterative method.

$$\begin{aligned}
\mathbf{W}_K^{(0)} &= \mathbf{W}_K^n \\
\mathbf{W}_K^{(j+1)} &= \mathbf{W}_K^{(0)} + \frac{\Delta t}{2}\mathbf{Q}(\mathbf{W}_K^{(j)}),\ j = 0, \ldots, \mathcal{M}-1 \\
\mathbf{W}_K^{(\mathcal{M}+1)} &= \mathcal{FV}(\mathbf{W}_K^{(\mathcal{M})}, \Delta t) \\
\mathbf{W}_K^{(j+1)} &= \mathbf{W}_K^{(\mathcal{M}+1)} + \frac{\Delta t}{2}\mathbf{Q}(\mathbf{W}_K^{(j)}),\ j = \mathcal{M}+1, \ldots, \mathcal{L} \\
\mathbf{W}_K^{n+1} &= \mathbf{W}_K^{(\mathcal{L}+1)}.
\end{aligned} \tag{20}$$

5 Examples of numerical results

5.1 Flow in a convergent-divergent nozzle

Consider transonic flow of steam in a nozzle (subsonic velocity at the inlet and the supersonic velocity at the outlet), see the Fig. 2(a). Presented case is defined by the Dirichlet boundary conditions at the inlet, given by the Table 1.

$p_{total,inlet}$	$T_{total,inlet}$	Q_0	Q_1	Q_2	χ_{inlet}
78390	373.1	0	0	0	0

Table 1: Inlet boundary conditions for the nozzle flow case.

The results have been obtained by the 1D version of the fully explicit code, taking into account the varying cross-sectional area. The main reason of choosing the 1D code is to focus attention on the flow model and to avoid additional numerical errors caused by multi-D domain discretization. The stopping criterion for the time marching method is the value of time derivative of $\mathbf{W}$, which goes to 'machine zero' for the 1D code. The domain has been discretized using 200 cells along the axis, the grid spacing in the convergent-divergent part of the domain is equal to $1.4 \cdot 10^{-3}$ and the time step has been set to $\Delta t = 1.2 \cdot 10^{-7}$. Figure 3 shows the comparison of four different flow models achieved by the L-W method. The correct position of nucleation start for models based on the perfect gas equation of state (the models AVG-P and DSDF-P) is achieved thanks to the correction (11). This correction is not applied for the models based on the virial equation of state (9), i.e. for the models AVG-V and DSDF-V. All models yield nearly the same distribution of pressure and wetness, see the Fig. 3. The best agreement with experimental data is achieved by the model DSDF-V. The models AVG-P and DSDF-P do not reach the local maximum of pressure at $x = 0.04\ m$. Nucleation starts for smaller x-values for the AVG-V model.

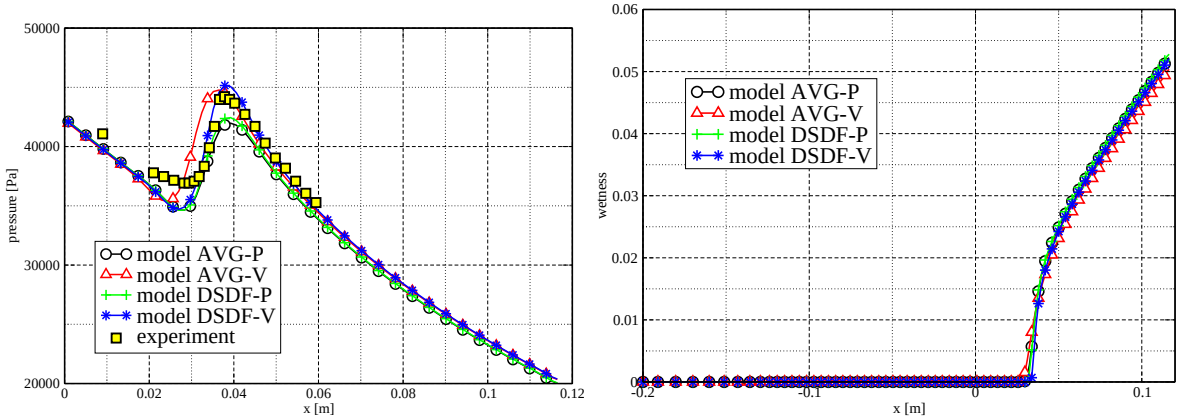

(a) detail of pressure in divergent part (b) wetness

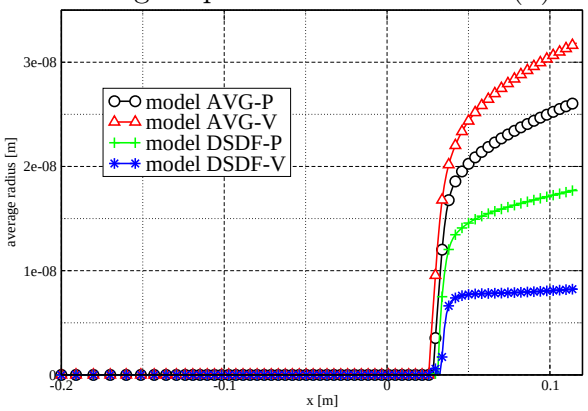

(c) droplet average radius

Figure 3: Results achieved by four presented models, experimental data from [3]

Significant difference between results achieved by all models can be observed in the average droplet size prediction, where the DSDF-V model yields the smallest and the AVG-V the biggest droplets. The results show relation between the average droplet size and the size of the pressure rise in the nucleation zone. Bigger pressure rise is most probably linked with higher nucleation rate J at the start of the nucleation, i.e. the mixture contains higher amount of smaller droplets. The average droplet size depends also on the position of the nucleation start, later start means higher sub-cooling of the vapor and therefore it is linked to smaller droplets. These observations are also consistent with numerical results published in [5], where earlier nucleation start, compared to our results, yields the outlet average droplet radius around $7 \cdot 10^{-8}$ m. Similar effect has the amount of numerical dissipation introduced by finite volume method $\mathcal{FV}$ used for the convection step (17). More dissipative methods yield smaller magnitude of pressure jump and the mixture therefore contains smaller amount of bigger droplets (i.e. bigger average radius), see the Fig. 4, where more dissipative Lax-Wendroff method yields the outlet average droplet radius around $3.5 \cdot 10^{-8}$ m and less dissipative CFFV and SRNH methods yields smaller outlet average droplet radius around $2.5 \cdot 10^{-8}$ m. All methods give nearly identical wetness.

Also an interesting observation is as follows. Additional grid refinement, which reduces numerical dissipation, leads to smaller droplets and has practically no effect on wetness. The wetness is relatively insensitive to all presented modifications of the flow model as well as of the numerical method, i.e. numerical simulation can provide relatively reliable prediction for wetness. It seems the droplet size prediction unfortunately strongly depends on the used model, method, grid etc.

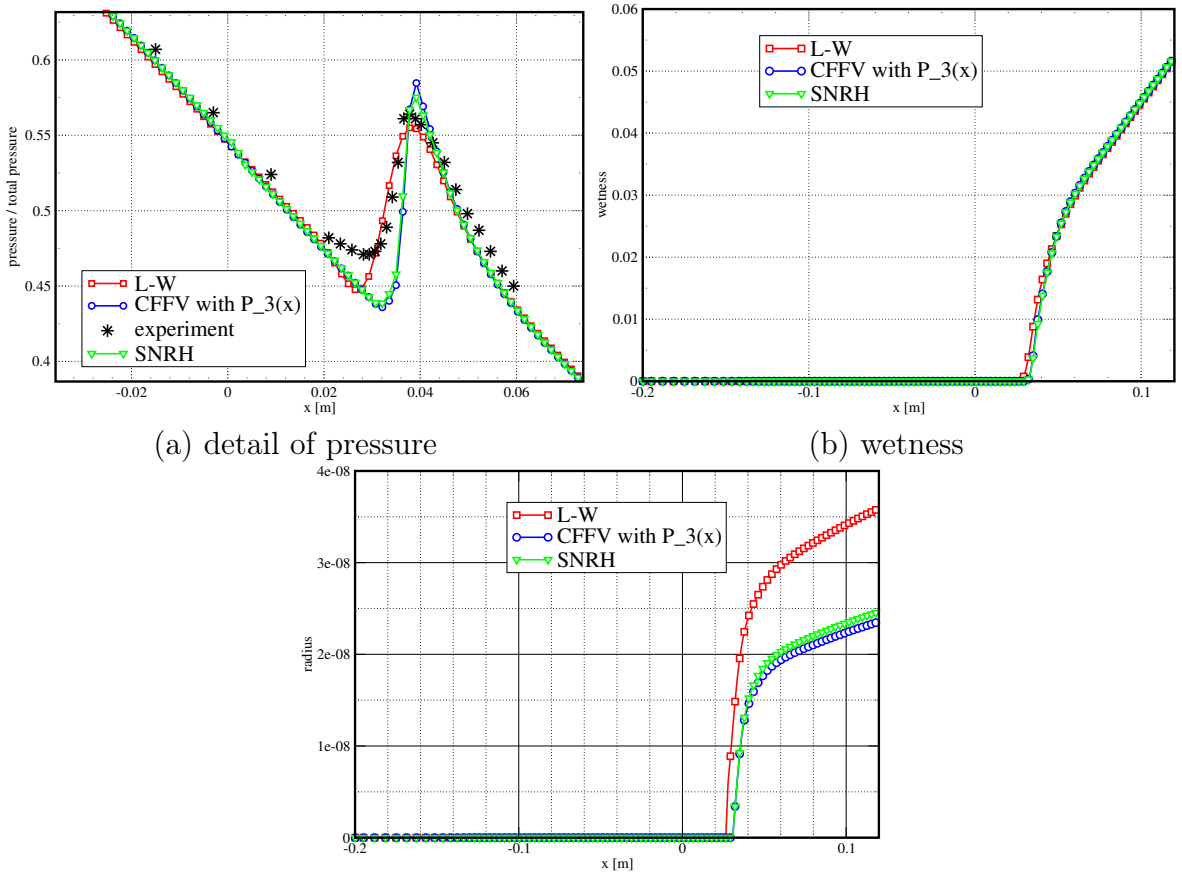

(a) detail of pressure

(b) wetness

(c) average droplet radius

Figure 4: Distributions along axis of Barschdorff nozzle [3], different numerical methods for AVG-P model.

5.2 Three-dimensional flow in a cascade

The results of three-dimensional two-phase flow in a stator cascade have been obtained by the numerical method with the implicit Euler method for the integration of source term and the AVG-P flow model. The computational grid consists of the single block of structured hexahedral grid with 91x25x18 points in downstream, tangential and span-wise directions, see the Fig. 5. We consider the constant inlet total temperature $T_{01} = 336\ K$, the constant inlet total pressure $p_{01} = 37534\ Pa$, zero inlet pitch angle, linear distribution of yaw angle between hub and tip casings and dry meta-stable steam at the inlet, i.e. zero inlet wetness and zero Hill's moments Q_i at the inlet. The outlet static pressure is a function of radial coordinate and is constant in circumferential direction. The effect of surface tension correction term (11) was published in [21].

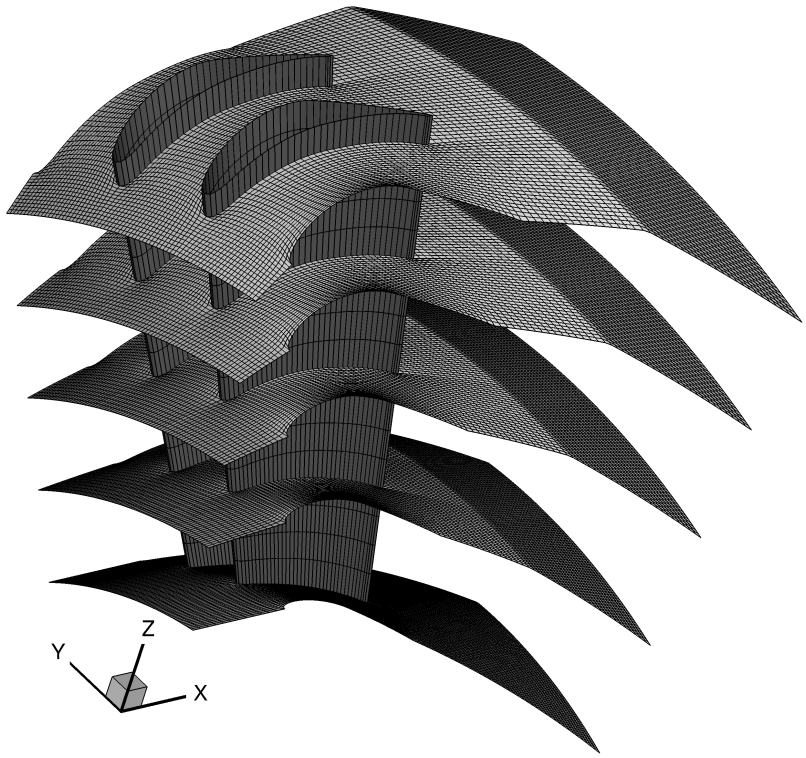

Figure 5: Computational grid for 3D stator cascade, several blade channels are plotted, computation is performed using only one blade channel.

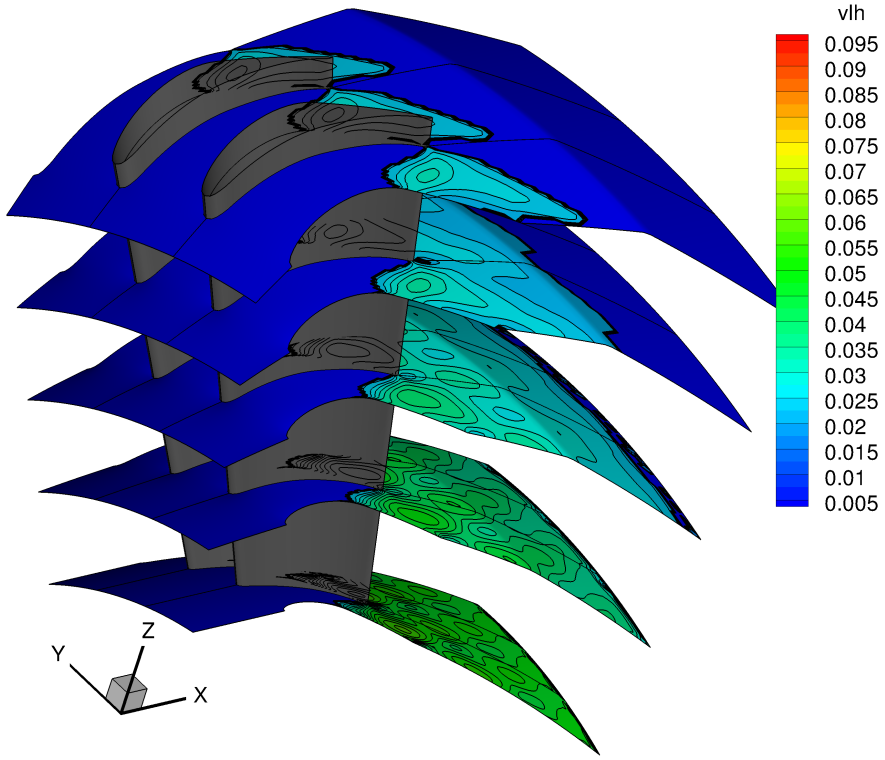

Figure 6: Wetness contours.

5.3 Unsteady stator rotor interaction

Numerical code for the three-dimensional single-phase unsteady stator/rotor interaction in an axial turbine cascade has been developed during cooperation with VKI. Extensive comparison of unsteady experimental data with unsteady numerical results for the BRITE stage was published in [26] and [22]. Another results for NASA core turbine stage were published in [20]. These simulations helped to fix boundary conditions for unsteady single phase flow. Implementation of AVG-P two-phase flow model into two-dimensional version of unsteady stator/rotor interaction code has brought the need to modify the outlet boundary condition. The condition of constant outlet pressure has been supplemented by the homogeneous Neumann condition for the temperature to avoid non-physical oscillations of wetness along the outlet boundary [23]. The last development of the code for the computation of unsteady two-dimensional two-phase flow in stator/rotor interaction has been aimed at extension for the cases with non-zero wetness of incoming steam. The droplet growth model has been regularized [25] to enhance the code robustness.

Following figures show example of unsteady flow of wet steam in turbine stage of low pressure part of turbine with wet steam already at the inlet. Figure 7 shows isolines of pressure in two consequent positions of rotor cascade during the rotor movement of one rotor pitch (the time necessary for the rotor shift of one pitch is denoted as τ_R). The flow field in the stator cascade does not contain shock waves, the pressure field between stator and rotor is without strong gradients. The structure of isolines for different rotor positions is therefore very similar. The following figures 8 - 10 show isolines of wetness, vapor sub-cooling and average droplet radius respectively.

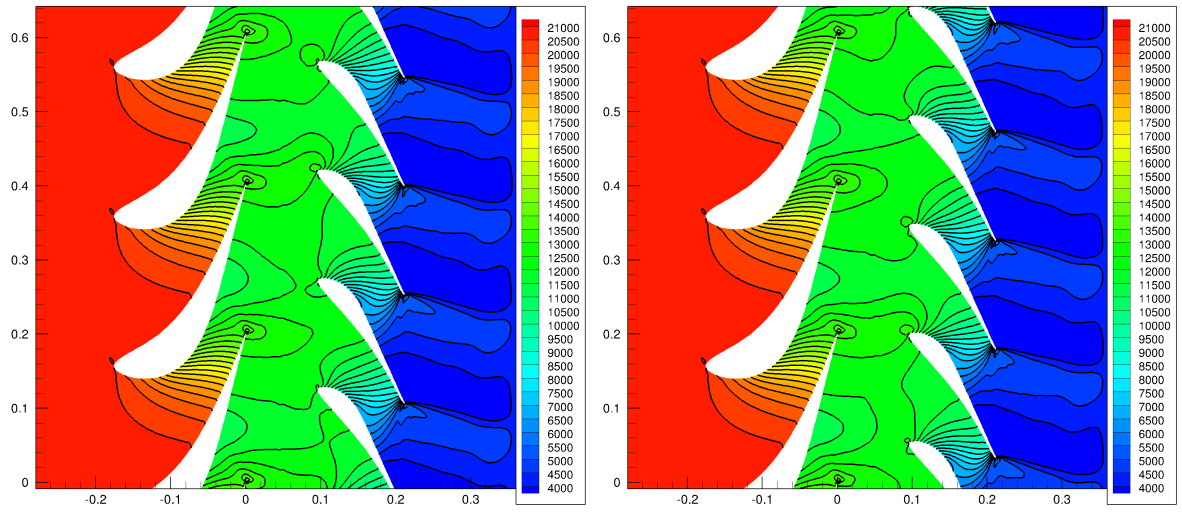

(a) $t = t_0$ (a) $t = t_0 + 0.5\tau_R$

Figure 7: Stator-rotor interaction - pressure field.

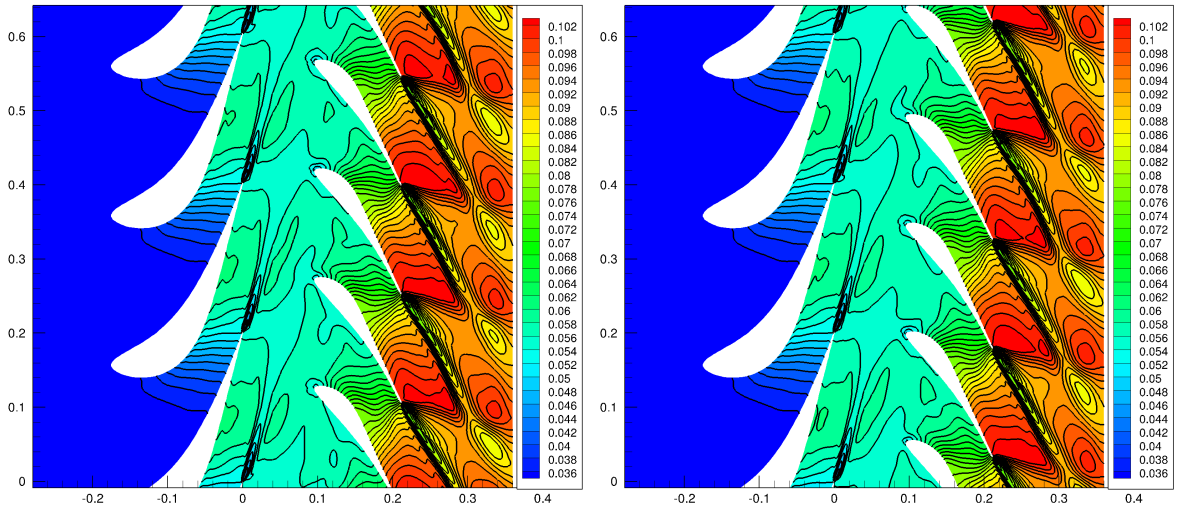

(a) $t = t_0$ (b) $t = t_0 + 0.5\tau_R$

Figure 8: Stator-rotor interaction - wetness.

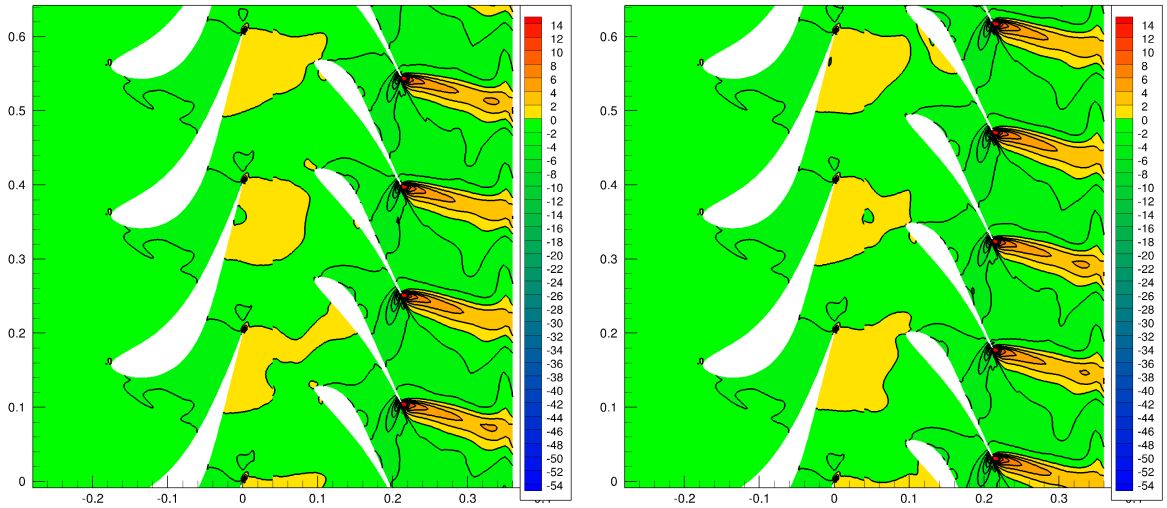

(a) $t = t_0$ (b) $t = t_0 + 0.5\tau_R$

Figure 9: Stator-rotor interaction - vapor temperature minus saturation temperature.

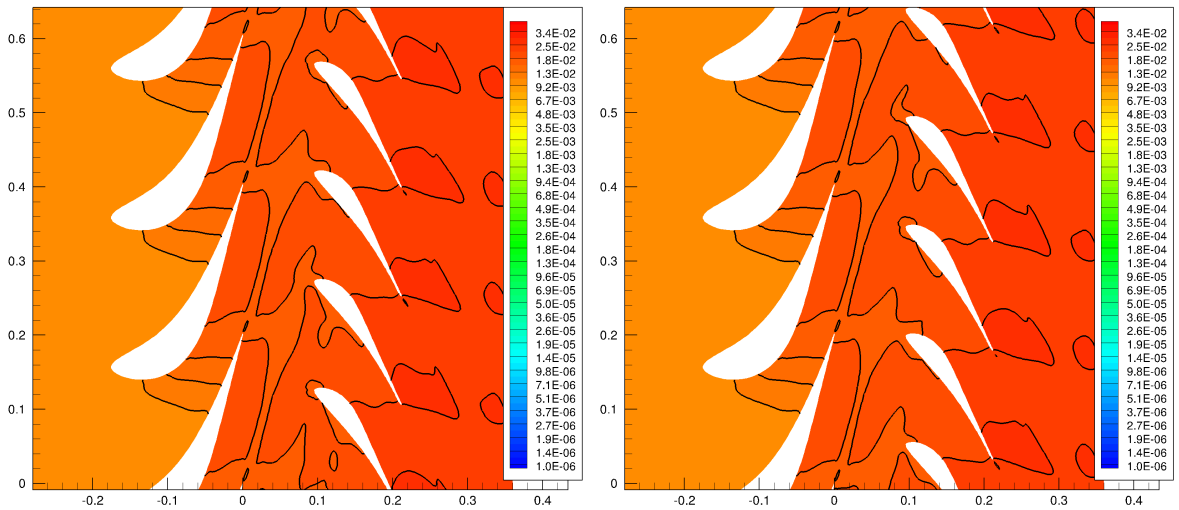

(a) $t = t_0$ (b) $t = t_0 + 0.5\tau_R$

Figure 10: Stator-rotor interaction - average droplet size $[\mu m]$.

6 Conclusions

The original model published in [17] has been substantially extended. Original numerical method based on the finite volume method (Lax-Wendroff, CFFV or SRNH) for the convection part and the Runge-Kutta or implicit Euler method for the production part has been developed. Modifications of flow model as well as modifications of numerical method have been verified for the case of transonic flow of condensing steam in the Barschdorff nozzle. This test case is characterized by the flow accelerating in the whole domain. The one-dimensional model with variable crossection has been used to avoid errors introduced by spatial discretization. Therefore all steady one-dimensional simulations converged to 'machine zero'. The effect of numerical dissipation on the wetness and the droplet size was published in [24] and [25]. Numerical method based on the Lax-Wendroff finite volume method has been successfully extended for the cases of two- and three-dimensional steady flow in a turbine cascade and results were published in [23] or [21]. Numerical code for the solution of unsteady stator/rotor interaction, which was initially developed for single-phase flow problems, details about this code are available in [26], [22] and [20], has been extended for two-phase flow of condensing steam. This extended code is based on the AVG-P model for two-phase flow, the Lax-Wendroff finite volume method and has modified outlet boundary condition for constant pressure with additional homogeneous Neumann condition for the temperature to avoid non-physical oscillations of wetness along the outlet boundary. First results of two-phase flow of condensing steam in unsteady stator/rotor interaction were published in [23]. Numerical method has been also recently extended for the cases with non-zero wetness of incoming steam and the droplet growth model has been regularized, details were published in [25].

References

[1] F. Bakhtar and A. K. Alubaidy. On the solution of supersonic blade-to-blade flows of nucleating steam by the time-marching method. In *IMechE conference on computational methods in turbomachinery*, pages 101–111, University of Birmingham, UK, 1984. Paper C82/84.

[2] F. Bakhtar and M. T. Tochai Mohammadi. An investigation of two-dimensional flow of nucleating and wet steam by the time-marching method. *Int. J. Heat Fluid Flow*, 2:5–18, 1980.

[3] D. Barschdorff. Verlauf der zustandgroesen und gasdynamische zuammenhaenge der spontanen kondensation reinen wasserdampfes in lavaldüsen. *Forsch. Ing.-Wes.*, 37(5), 1971.

[4] R. Becker and W. Döring. Kinetische behandlung der keimbildung in übersättingten dämpfen. *Ann. d. Physik*, 24(8), 1935.

[5] S. Dykas. Numerical calculation of the steam condensing flow. *Task Quarterly*, 4:519–535, 2001.

[6] S. Dykas, K. Goodheart, and G. H. Schnerr. Numerical study of accurate and efficient modelling for simulation of condensing flow in transonic steam turbines. In *5th European conference on Turbomachinery*, pages 751–760, 2003. Praha.

[7] A. G. Gerber and M. J. Kermani. A pressure based eulerian–eulerian multi-phase model for non-equilibrium condensation in transonic steam flow. *International Journal of Heat and Mass Transfer*, 47:2217–2231, 2004.

[8] M. Heiler. *Instationäre Phänomene in homogen/heterogen kondensierenden Düsen- und Turbinenströmungen.* PhD thesis, Uni Karlsruhe, 1999.

[9] P. G. Hill. Condensation of water vapor during supersonic expansion in nozzles. *Journal of Fluid Mechanics*, 3:593–620, 1966.

[10] V. John, I. Angelov, A. Önc'ül, and D. Thevenin. Techniques for the reconstruction of a distribution from a finite number of its moments. *Journal Chemical Engineering Science*, 62(11):2890–2904, 2007.

[11] M. Moheban and J. B. Young. A time-marching method for the calculation of blade-to-blade non-equilibrium wet steam flows in turbine cascades. In *IMechE conference on computational methods in turbomachinery*, pages 89–99, University of Birmingham, UK, 1984. Paper C76/84.

[12] A. Mousavi, A. G. Gerber, and M. J. Kermani. Representing polydispersed droplet behavior in nucleating steam flow with the quadrature - method - of - moments. In *2006 ASME Joint U.S.-European Fluids Engineering Summer Meeting*, 2006.

[13] V. Petr and M. Kolovratník. Heterogenous effects in the dropplet nucleation process in lp steam turbines. In *4th European Conference on Turbomachinery*, Firenze, Italy, 2001.

[14] M. Šejna and J. Lain. Numerical modelling of wet steam flow with homogenous condensation on unstructured triangular meshes. *Journal ZAMM*, 74(5):375–378, 1994.

[15] G. Strang. On the construction and comparison of difference schemes. *SIAM Journal of Numerical Analysis*, 5:506–517, 1968.

[16] L. Sun, Q. Zheng, and S. Liu. 2d-simulation of wet steam flow in a steam turbine with spontaneous condensation. *Journal of Marine Science and Application*, 6(2):59–63, 2007.

[17] M. Šťastný and M. Šejna. Condensation effects in transonic flow through turbine cascade. In *Proceedings of the 12th international conference of the properties of water and steam*, pages 711–719. Begel House, 1995.

[18] W. Wroblewski, S. Dykas, and T. Chmielniak. Models for water steam condensing flows. *Archives of Thermodynamics*, 33(1):67–86, 2012.

[19] J. B. Young. Two-dimensional, nonequilibrium, wet-steam calculations for nozzles and turbine cascades. *Journal of Turbomachinery*, 114:569–579, 1992.

[20] J. Dobeš, J. Fořt, J. Fürst, J. Halama, and K. Kozel. Numerical modeling of unsteady flow in steam turbine cascade. *Journal of Computational and Applied Mathematics*, 234(7):2336–2341, 2010. ISSN 0377-0427.

[21] J. Halama. Transonic flow of wet steam - numerical simulation. *Acta Polytechnica*, 52(6):124–130, 2012.

[22] J. Halama, T. Arts, and J. Fořt. Numerical solution of steady and unsteady transonic flow in turbine cascades and stages. *Computers and Fluids*, 33(5-6):729–740, 2003.

[23] J. Halama, F. Benkhaldoun, and J. Fořt. Numerical modeling of two-phase transonic flow. *Journal Mathematics and Computers in Simulation*, 80(8):1624–1635, 2010. ISSN 0378-4754.

[24] J. Halama, F. Benkhaldoun, and J. Fořt. Flux schemes based finite volume method for internal transonic flow with condensation. *International Journal for Numerical Methods in Fluids*, 65(8):953–968, 2011.

[25] J. Halama and J. Fořt. Numerical simulation of two-phase flow in a low pressure steam turbine stage. *Journal Computing*, 2013. DOI: 10.1007/s00607-013-0292-6.

[26] E. Valenti, J. Halama, R. Dénos, and T. Arts. Investigation of the 3d unsteady rotor pressure field in a hp turbine stage. In *Proceedings of of ASME TURBO EXPO 2002*, Amsterdam, June 2002. ASME. ASME Paper GT-2002-30365.

Ing. Jan Halama, Ph.D.

Narozen 15. listopadu 1972 v Praze. V roce 1991 maturoval na gymnáziu Korunní se zaměřením na matematiku. V roce 1996 ukončil magisterské studium na Fakultě strojní, ČVUT v Praze, obor Aplikovaná mechanika. V roce 1998 absolvoval Diploma course, VKI, Belgie (roční po-magisterský kurz se zaměřením na mechaniku tekutin), práce "Numerical study of the unsteady stator/rotor interaction" byla oceněna Cenou belgické vlády a cenou za nejlepší prezentaci. V roce 2003 získal titul Ph.D. v oboru Matematické a fyzikální inženýrství, dizertační práce na téma Numerické řešení proudění v turbínových mřížích a stupních.

J. Halama se zabývá numerickými simulacemi jednofázového i dvoufázového proudění stlačitelné tekutiny zvláště v turbostrojích. Vyvíjí vlastní výpočtové programy pro řešení stacionárního i nestacionárního proudění vzduchu a mokré páry s kondenzací. Absolvoval několik zahraničních stáží ve VKI Rhode-Saint-Genese, ILR Uni Dresden, LAGA Uni Paris 13 a CMLA ENS Cachan. Spolupracuje s výzkumnými pracovišti ÚT AVČR a VZLÚ. Podílí se na spolupráci s průmyslovými podniky PBS Velká Bíteš a Škoda Power Plzeň. Byl a je členem řešitelských kolektivů grantů GAČR, MPO a MŠMT. Výraznou měrou se zasloužil o navázání spolupráce mezi ústavem technické matematiky a VKI a LAGA Uni Paris 13. V roce 2011 byl jedním z hlavních organizátorů mezinárodní konference FVCA6. Je členem redakční rady časopisu IJFV. Je zakládajícím členem mezinárodní asociace VKI-AA. Recenzuje články pro časopisy IJNMF (Wiley), ACM (KME ZČU Plzeň). Je autorem cca 60 prací, z toho 6 článků v impaktovaných časopisech (4 za posledních 5 let), 8 článků v mezinárodních recenzovaných časopisech (1 za posledních 5 let), v databázi WoS je indexováno 13 článků (5 za posledních 5 let) a 6 citací (4 za posledních 5 let).

J. Halama se zapojil do výuky na ústavu technické matematiky v roce 1997. Postupně cvičil a později i přednášel většinu povinných předmětů ústavu technické matematiky v bakalářském programu. Postupně se zapojil i do přednášek a cvičení jak v magisterském studijním programu (předměty NOPR, MAME, AMM), tak i v doktorském studijním programu (česká i anglická výuka předmětu Integrální a diskrétní transformace). Je spoluautorem skript. Vedl jednu bakalářskou a dvě diplomové práce. Působil jako školitel specialista u tří disertačních prací. Podílí se pravidelně na státních závěrečných zkouškách u dalších doktorských oborů FS ČVUT. Od roku 2005 zastává funkci tajemníka ústavu a organizuje pedagogickou činnost ústavu.